

DRAMatic Speedup: Accelerating HE Operations on a Processing-in-Memory System

Niklas Klinger¹, Jonas Sander¹, Peterson Yuhala², Pascal Felber² and Thomas Eisenbarth¹

¹ University of Luebeck, Germany

² University of Neuchâtel, Switzerland

Abstract. Homomorphic encryption (HE) is a promising technology for confidential cloud computing, as it allows computations on encrypted data. However, HE is computationally expensive and often memory-bound on conventional computer architectures. Processing-in-Memory (PIM) is an alternative hardware architecture that integrates processing units and memory on the same chip or memory module. PIM enables higher memory bandwidth than conventional architectures and could thus be suitable for accelerating HE. In this work, we present DRAMatic, which implements operations foundational to HE on UPMEM’s programmable, general-purpose PIM system, and evaluate its performance. DRAMatic incorporates many arithmetic optimizations, including residue number system and number-theoretic transform techniques, and can support the large parameters required for secure homomorphic evaluations. To compare performance, we evaluate DRAMatic against Microsoft SEAL, a popular open-source HE library, regarding both runtime and energy efficiency. The results show that DRAMatic significantly closes the gap between UPMEM PIM and Microsoft SEAL. However, we also show that DRAMatic is currently constrained by UPMEM PIM’s multiplication performance and data transfer overhead. Finally, we discuss potential hardware extensions to UPMEM PIM.

Keywords: Homomorphic Encryption (HE) · Processing-in-Memory (PIM) · Number-theoretic Transform (NTT)

1 Introduction

Data security is becoming increasingly important as more applications rely on cloud computing, especially in areas such as healthcare, where confidentiality and privacy of sensitive data is critical. Homomorphic encryption (HE) allows computations to be performed on encrypted data without decrypting it and without revealing any information about the inputs and outputs of the computation apart from their lengths. The results can be decrypted using the secret key corresponding to the original encrypted data. Current HE schemes rely on noise which is added to the encrypted data. When performing computations on this data, the noise compounds, which poses a limit on how many operations can be performed, as too much noise makes the results impossible to decrypt. Fully homomorphic encryption (FHE) solves this problem by introducing a special noise-reducing operation called bootstrapping. FHE allows arbitrary sequences of operations to be performed on the encrypted data, as long as bootstrapping is performed at appropriate times.

E-mail: n.klinger@uni-luebeck.de (Niklas Klinger), j.sander@uni-luebeck.de (Jonas Sander), peterson.yuhala@unine.ch (Peterson Yuhala), pascal.felber@unine.ch (Pascal Felber), thomas.eisenbarth@uni-luebeck.de (Thomas Eisenbarth)



Because HE allows us to perform computations on encrypted data, it can significantly enhance security in cloud computing contexts. Using HE, even highly sensitive computations can be outsourced to cloud providers or other third parties, because the data can stay encrypted throughout the whole process. Compared to Trusted Execution Environments (TEEs), HE provides pure cryptographic security guarantees and does not require trusting the TEE hardware used by a cloud provider. Additionally, the secret key stays on the client side and is thus not exposed to potential side-channel attacks in the cloud. Past research has revealed many such side-channels vulnerabilities in TEEs [MIE17, WSE24, CSB⁺26], making this a significant advantage for HE.

However, the main drawbacks of HE are its high memory and compute requirements compared to working directly on the unencrypted data. In traditional computer architectures, HE can also become bottlenecked by memory accesses, because HE operations have comparatively low *arithmetic intensity* [dCAY⁺21], meaning that they access a lot of data, but perform few arithmetic operations on each piece of data. Processing-in-Memory (PIM) is a hardware architecture that integrates processing units and memory on the same chip or memory module [GBK¹⁹]. It enables low-latency, high-bandwidth memory access compared to traditional architectures, in which processing units and memory are separated. PIM could thus be suitable for accelerating memory-intensive workloads like HE. While other work has mostly explored custom PIM designs [GR21, ZNG⁺25], we will focus on the general-purpose PIM system developed by UPMEM [GHF⁺21]. UPMEM PIM is programmable, highly parallel and provides high total memory bandwidth, but it also presents new challenges like overcoming the weak multiplication performance of the individual Data Processing Units (DPUs) and minimizing the communication costs between them. In this work, we implement typical HE operations on the general-purpose UPMEM PIM system and compare its performance with other implementations.

1.1 Our Contribution

We present DRAMatic, which implements typical HE operations on UPMEM PIM, namely BGV multiplication [BGV12], number-theoretic transforms (NTT), and inverse transforms (iNTT) [SSM⁺23]. To implement BGV multiplication efficiently, we optimize polynomial operations on UPMEM PIM, utilizing Residue Number Systems (RNS), NTT, Barrett reduction [Bar87], custom multiplications and careful buffering to speed-up modular polynomial multiplication.

Compared to previous work on accelerating HE with UPMEM PIM [MHY⁺24], we achieve a 334 times speed-up and support larger parameter sizes, that allow secure homomorphic evaluations in practical use-cases. Unlike concurrent work on accelerating NTT execution on UPMEM PIM [BMP⁺26], DRAMatic does not rely on expensive inter-DPU communication and scales better regarding the number of DPUs in the system. We also utilize smaller RNS moduli, thus avoiding large integer arithmetic and enabling optimized multiplication routines. Finally, DRAMatic is not limited to (i)NTT, but supports multiple operations, including modular addition and modular multiplication (polynomial or pointwise), NTT, and iNTT, which can be composed into larger operations like BGV multiplication.

Additionally, we compare the performance between DRAMatic and an optimized HE implementation on CPUs, significantly closing the gap compared to previous work [MHY⁺24]. We also show that the data transfer overhead and weak multiplication performance of DPUs remains a bottleneck for DRAMatic and discuss potential solutions in the form of hardware extensions to UPMEM PIM. Finally, we perform the first power measurements of UPMEM PIM for HE operations and compare the energy efficiency of DRAMatic with an optimized CPU implementation. Our implementation of DRAMatic is

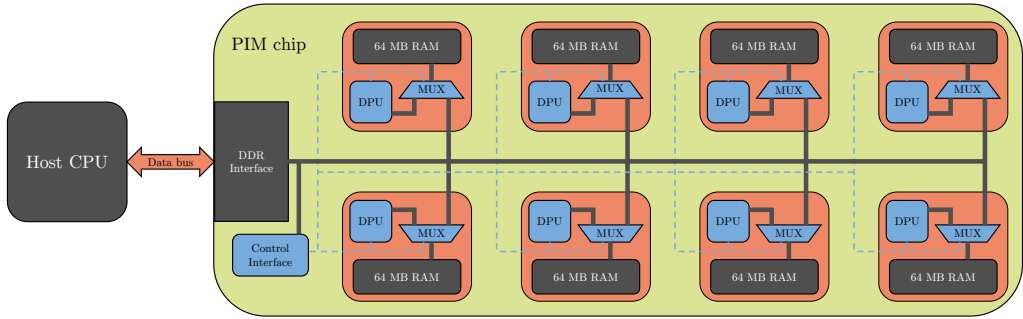


Figure 1: Architecture of an UPMEM PIM chip. Inspired by [UPM24].

open source¹.

2 Background

We now go into more detail on UPMEM PIM and HE.

2.1 UPMEM PIM

UPMEM PIM is a programmable near-memory computing architecture in which simple, general-purpose processors, called Data Processing Units (DPUs), are co-located with DRAM chips on special memory modules (PIM DIMMs). The DPUs are custom 32-bit RISC processors running at up to 400 MHz. They support 16 independent threads² and up to 11 of these threads can run concurrently at any given time. Each PIM DIMM has a total capacity of 8 GB and contains 128 DPUs on multiple PIM chips, with each DPU having access to a 64 MB slice of the module's main RAM (MRAM). Figure 1 shows the architecture of such an UPMEM PIM chip. Current UPMEM platforms support up to 20 PIM DIMMs, for a total of 2560 DPUs and a capacity of 160 GB.

DPUs can communicate with the host CPU via the DDR interface. Inter-DPU communication is not possible directly and must go through the host CPU instead, meaning that the data must first be copied from one DPU to the CPU's main memory and then copied from the main memory to another DPU. This process is slow, as it requires synchronization between all three components. Frequent inter-DPU communication should thus be avoided, which we need to consider when implementing HE operations. The CPU can also not use the DPUs' memory directly. Instead, it must use normal DRAM for its computations and then copy the data to the PIM DIMMs when required.

Although DPUs are connected to 64 MB of MRAM, they can only directly access an additional, smaller memory, called the working memory (WRAM), of which each DPU has 64 KB. Special direct memory access (DMA) instructions are used to transfer data between the WRAM and MRAM of a DPU. Since the memory of individual DPUs is limited, we will need to split data and inputs over multiple DPUs when implementing HE operations on UPMEM PIM.

The native word size of DPUs is 32-bit, but the DPU hardware does not directly support 32x32-bit or even 16x16-bit integer multiplications. The hardware multiplier can only perform 8x8-bit multiplications, which yield 16-bit results. Larger multiplications thus need to be constructed out of multiple instructions. As implemented by the DPU

¹<https://github.com/UzL-ITS/DRAMatic-Speedup>

²These capabilities refer to the v1B DPU model. UPMEM also provides a v1A model with slight differences. See https://sdk.upmem.com/2025.1.0/03_ProgrammingWithUpmemDpu.html#dpu-chip-characteristics.

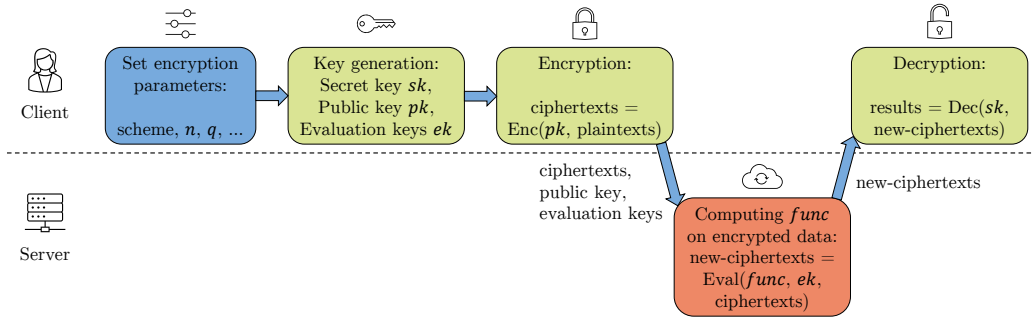


Figure 2: Steps in the usage of an HE scheme, showing the roles of client and server.

compiler, 32-bit multiplications are up to 43 times slower than 8-bit multiplications; and 64-bit multiplications are 134 times slower. This poses a challenge when implementing HE operations, which often involve big coefficients (hundreds of bits). The DPUs also do not have hardware supported floating point operations; they are implemented in software instead, which results in poor performance. As such, floating point operations should be avoided for most applications. This also means that optimized HE variants like [HPS19] which rely on floating-point arithmetic, cannot be used on UPMEM PIM.

DPUs feature a 14-stage pipeline, but the three first and last stages of dependent instructions can execute in parallel [GHF⁺21]. Thus, only 11 active threads are needed to fully saturate the pipeline. Active threads are scheduled in a round-robin way; with threads considered active unless they are explicitly waiting (*e.g.*, on a mutex) or performing a DMA operation. These DMA operations execute sequentially; and threads waiting on a DMA operation are placed in a special queue. Thus, only one thread of each DPU can access the MRAM at any given time.

2.2 HE Schemes

Current practical HE schemes are based on the Learning With Errors (LWE) or Ring Learning With Errors (RLWE) problem and use noisy polynomials as ciphertexts. RLWE based HE schemes like BFV [Bra12, FV12] and BGV [BGV12] operate on polynomial rings denoted as $\mathbb{Z}_q[x]/(x^n + 1)$, *i.e.*, the ring of integer polynomials modulo the polynomial $x^n + 1$ and with coefficients modulo q (other rings are possible, but this is the most popular choice). Ciphertexts then consist of two or more such polynomials. The two main operations on ciphertexts, which make the schemes homomorphic, require polynomial addition and polynomial multiplication. It may also be required to perform polynomial modulus and coefficient modulus operations, to ensure that the ciphertexts stay within the relevant polynomial ring. Other HE schemes like Torus Fully Homomorphic Encryption (TFHE) [CGGI20] or CKKS [CKKS17] also exist, but are not the focus of this work.

2.2.1 Steps in an HE Scheme

Usage of an HE scheme can be logically split into the following steps: parameter selection, key generation, encryption, computation, and decryption, as shown in Figure 2. In this work, we consider a scenario in which a client wants to offload computations to an untrusted server (*e.g.*, a cloud service provider) using HE. This means that key generation, encryption, and decryption are performed by the client, while the server handles computations on the encrypted data and potentially negotiates encryption parameters with the client. Our focus is the computation on encrypted data, which corresponds to the server side of this interaction.

2.2.2 BGV

For our evaluation, we focus on the BGV multiplication. In BGV, two ciphertexts $ct = (ct_0, ct_1)$ and $ct' = (ct'_0, ct'_1)$, are multiplied to produce $ct_{res} = (c_0, c_1, c_2)$ as follows:

$$\begin{aligned} c_0 &= [ct_0 \cdot ct'_0]_{q_l} \\ c_1 &= [ct_0 \cdot ct'_1 + ct_1 \cdot ct'_0]_{q_l} \\ c_2 &= [ct_1 \cdot ct'_1]_{q_l} \end{aligned}$$

where $[\cdot]_{q_l}$ is a modular reduction by the current modulus level, which can change through a process called *modulus switching*. In BGV, modulus switching improves the performance of the scheme and is done when ciphertexts become too noisy after a series of operations.

Note that the BGV multiplication does not involve scaling or rounding operations as in other schemes like BFV. When we combine BGV with RNS, this means that all operations required for BGV multiplication can be performed on the individual residues independently from each other. BGV multiplication is thus well suited for implementing on UPMEM PIM, as it allows us to split a multiplication over multiple DPUs using RNS, which we describe below.

3 Design Considerations

In the following, we discuss the challenges of efficiently implementing BGV operations on UPMEM PIM DPUs.

3.1 Large Coefficients

To efficiently operate on the large coefficients of HE ciphertexts, we use a RNS representation for the ciphertext polynomials. An RNS enables the decomposition of large integers into several smaller residues, each computed modulo a distinct base. In this representation, a large modulus M is expressed as the product of smaller pairwise coprime moduli m_1, m_2, \dots, m_k , called the RNS base. Each coefficient x modulo M is then represented by the tuple of its residues

$$(x_1, x_2, \dots, x_k), \quad \text{where } x_i = x \bmod m_i.$$

Addition and multiplication can now be performed independently on each residue, *i.e.*,

$$(x \circ y) \bmod M \longleftrightarrow (x_1 \circ y_1 \bmod m_1, x_2 \circ y_2 \bmod m_2, \dots, x_k \circ y_k \bmod m_k),$$

where \circ denotes either addition or multiplication. The original value modulo M can be reconstructed from its residues using the Chinese Remainder Theorem (CRT):

$$x \equiv \sum_{i=1}^k x_i M_i N_i \pmod{M},$$

where $M_i = M/m_i$ and N_i is the modular inverse of M_i modulo m_i . For the mathematical background, we refer the reader to works on number theory and algebra, *e.g.*, [Sho05].

Crucially, RNS enables us to do computations modulo M , by operating on smaller numbers moduli m_i . Because DPU multiplication and modulus performance is limited, we want the individual residues to be as small as possible. For our use-case, this results in 32-bit residues, which is also the DPUs' native word size. 16-bit residues would be even faster, but they cannot be combined with NTT, as there aren't enough suitable primes smaller than 16-bit (see Subsubsection 3.2.1). Additionally, we implement a custom 32-bit multiplication routine, which is faster than the compiler generated one for our use-case and reduces the speed difference between 32-bit multiplication and 16-bit multiplication.

```

fn custom_mul_32to64(a, b):
    a0, a1 = split(a, 16)
    b0, b1 = split(b, 16)
    lo = a0 * b0
    m1 = a0 * b1
    m2 = a1 * b0
    hi = a1 * b1
    // combine results
    return hi << 32 +
        (m1 + m2) << 16 + lo

```

Listing 1: Pseudocode of our custom 32-bit to 64-bit multiplication routine. Combining the results is done in hand-written assembly for increased performance.

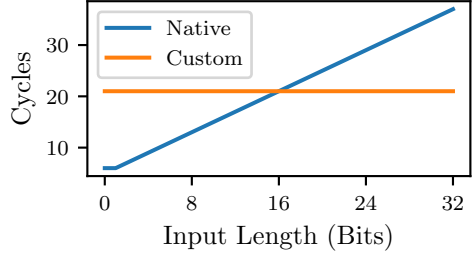


Figure 3: Runtime of our custom 32-bit to 32-bit multiplication and the native DPU implementation for different input sizes.

3.1.1 Custom Multiplication Routines

We improve multiplication performance by implementing custom 32-bit multiplication routines on the DPUs. While we can limit our inputs to 32-bit using RNS, we still need 64-bit intermediate results to correctly perform modular reductions. When using native arithmetic as implemented by the DPU compiler, we have to perform full 64-bit multiplications to get correct results, even though our inputs are only 32-bit values. Our custom multiplication routine instead constructs the result by appropriately shifting and adding the results of four native 16x16-bit multiplications, as shown in Listing 1. This straightforward routine takes 35 cycles and is about 70% faster than the native full 64-bit multiplication. We also tested a Karatsuba implementation to reduce the number of 16x16-bit multiplications to three, but this is actually 4 cycles slower, as the additional overhead for combining the results is more significant than the saved multiplication.

Similarly, we also implement custom 32-bit multiplication that only produces 32-bit results. In that routine, we skip the `hi`-computation from Listing 1 and simplify the computations of `m1` and `m2`, as their upper bits are unused, which reduces the runtime to 21 cycles. Note that the runtime of the native 32-bit multiplication with 32-bit results depends on the highest set bit in its inputs. The native implementation makes a compromise: it is optimal for small inputs, which are typical in many applications, but is relatively slow in the worst case. Our custom multiplication routine has constant runtime instead. The result is shown in Figure 3; our implementation is faster when both factors are longer than 16 bits, but is otherwise slower than the native implementation. However, this is still an improvement for our use-case; since we are operating on encrypted data, large input values are common, as the data is seemingly random.

3.1.2 Barrett Reduction

To further speed up modular multiplication, we utilize Barrett reduction, which is optimized for repeated reductions by the same modulus and was first introduced by Barrett [Bar87] for a fast RSA implementation. Given v and m , consider that we want to find the remainder $x = v \bmod m$. The idea of Barrett reduction is to pre-compute a scaled reciprocal $R = \lfloor 2^n/m \rfloor$ of the modulus. The remainder can then be approximated as $x \approx v - m \cdot \lfloor vR/2^n \rfloor$ and can be corrected with a final conditional subtraction. In essence, we exchange the original division for two multiplications, a bit shift and a conditional subtraction, which is much faster on DPUs. In DRAMatic, the *Barrett factor* R of every modulus is pre-computed by the CPU and then transferred to the appropriate DPUs.

3.2 Large Polynomials

The usage of RNS representations, Barrett reduction, and our custom multiplication routine already speeds up the multiplication of individual coefficients, but the large polynomial multiplications used in HE must also be optimized. Recall that a naive polynomial multiplication requires $\mathcal{O}(n^2)$ steps. To improve polynomial multiplication performance, we utilize negacyclic NTT [SSM⁺23], which is a generalization of the discrete Fourier transform (DFT) to a finite field. After performing NTT, polynomial multiplications (and additions) can be performed pointwise, *i.e.*, in linear time. An inverse NTT (iNTT) can then be performed to get the resulting polynomial back into coefficient form. More formally, given two polynomials A and B from the polynomial ring $\mathbb{Z}_q[x]/(x^n + 1)$, it holds that

$$A \cdot B = \text{iNTT}(\text{NTT}(A) \circ \text{NTT}(B))$$

where \cdot is modular polynomial multiplication and \circ is modular pointwise multiplication. Since both NTT and iNTT, can be applied in $\mathcal{O}(n \log n)$ time, the total time required for polynomial multiplication using NTT is reduced to $\mathcal{O}(n \log n)$.

As NTT is a generalization of the DFT, many fast DFT algorithms can also be adapted to it, like the Cooley-Tukey fast Fourier transform [CT65] and many of its variations. To speed-up polynomial multiplication on DPUs, we implement fast NTT and iNTT with bit-reversed outputs, based on Cooley-Tukey and Gentleman-Sande [GS66] butterflies. The idea behind these algorithms is a divide and conquer approach, as the NTT of a length n polynomial can be computed from the NTTs of its two parts with length $n/2$. In practice, the algorithms require $\log_2(n)$ passes over the data (stages), in which so-called butterflies are applied to pairs of coefficients. A visualization of the NTT butterfly stages is shown in Figure 4. Because of the butterflies' crossing pattern, the output of the final NTT or iNTT stage is produced in bit-reversed order. For example, on the right of Figure 4, output $t_4 = t_{100_2}$ is actually in the $\text{reverse}(100)_2 = 001_2 = 1$ st position (counting from 0 at the top). This bit-reversed order can be corrected by an additional reordering-pass. However, BGV multiplication only requires polynomial addition and polynomial multiplication, which are pointwise operations after an NTT. Thus, the order of elements is irrelevant for these operations (as long as it is consistent) and we skip the additional reordering pass as an additional optimization. Computations are thus performed in bit-reversed order and the results are then reversed again by the final iNTT. Lastly, these NTTs take so-called twiddle factors as additional inputs, which are pre-computed powers of a root-of-unity ψ , as seen in Figure 4. In DRAMatic, these twiddle factors are pre-computed by the CPU and then transferred to the DPUs.

3.2.1 Combining RNS and NTT

To combine RNS and NTT, we split the coefficients of the ciphertext polynomials using RNS and then perform NTT on the groups of residues which share a modulus, which we also call sub-polynomials. The polynomials are stored as multiple sub-polynomials and each sub-polynomial is continuous in memory. In other words, the polynomials are stored in a *tuple of arrays of residues* layout. Compared to an *array of tuples of residues* layout, this provides more flexibility in distributing the data between DPUs or DPU threads and simplifies the iteration over residues of the same modulus, because they are continuous in memory. See Figure 5 for an illustration.

Note that NTT requires a prime working modulus p , which satisfies $p = 2n + 1$ (where n is the length of the polynomials). This sets a minimum size on the RNS residues, as for typical HE polynomial lengths, *e.g.*, $n = 4096$, there aren't enough such primes smaller than 16-bit. We thus use 32-bit residues in DRAMatic.

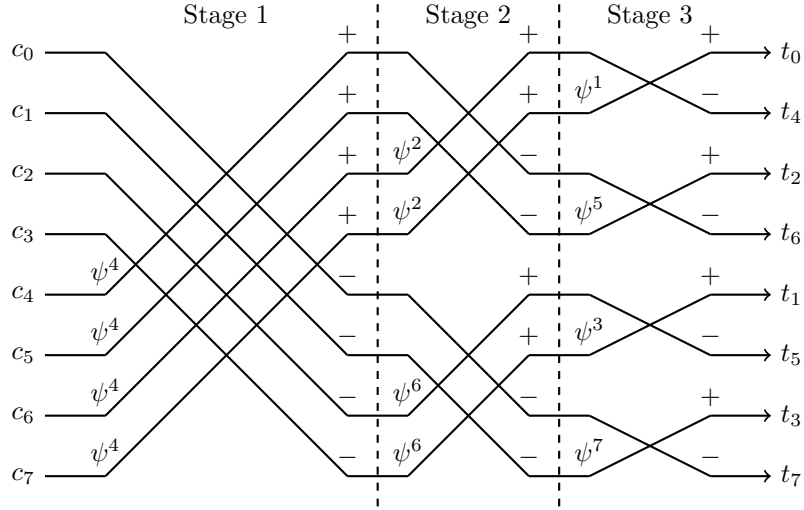


Figure 4: Visualization of NTT butterflies. Shown for $n = 8$ with $\log_2(n) = 3$ stages.

3.3 Splitting Work over DPUs

We split the coefficient data over DPUs based on its residues, which allows us to parallelize work (even for single ciphertext pairs) while avoiding inter-DPU communication. Each DPU gets configured for a particular modulus of the RNS base and then only operates on sub-polynomials of that modulus. For example, consider an RNS base (m_1, m_2, m_3) . Each polynomial of a ciphertext ct would thus consist of three sub-polynomials:

$$ct = (ct_0, ct_1) = ((ct_0^{m_1}, ct_0^{m_2}, ct_0^{m_3}), (ct_1^{m_1}, ct_1^{m_2}, ct_1^{m_3}))$$

One third of the available DPUs would then be configured for modulus m_1 and operate only on sub-polynomials $ct_0^{m_1}$ and $ct_1^{m_1}$ of a particular ciphertext. Another third would be configured for modulus m_2 and thus operate on $ct_0^{m_2}$ and $ct_1^{m_2}$, while the last third would be configured for modulus m_3 . Another advantage of this split is that each DPU only has to operate on a single modulus and thus only needs support data (like NTT twiddle factors) for this one modulus, which reduces the memory requirements for the DPUs.

3.4 Other Considerations

To optimize the memory layout of iNTT twiddle factors, we store them in a different, *scrambled* order, similar to Microsoft SEAL [SEA23]. To be precise, the i -th inverse root of unity power ψ^{-i} is stored in position $1 + \text{bit_reverse}(i - 1)$, which closely matches the access patterns of our iNTT implementation on DPUs. This order ensures that both the polynomial data and the twiddle factors are always accessed sequentially in memory, which allows for more effective buffering in DPU WRAM and thus improves performance. With this scrambled order, we measured a 1.27 times speed-up compared to storing the twiddle factors in logical order.

We differentiate between coarse-grained and fine-grained multithreading on DPUs. In fine-grained multi-threading, multiple DPU threads operate on the same sub-polynomials simultaneously. This can improve performance even with few sub-polynomials. In coarse-grained multithreading, each DPU thread operates on its own sub-polynomials independently from other threads. For the maximum performance improvement, this type of multi-threading requires the DPU to operate on many sub-polynomials concurrently. We use fine-grained multi-threading for element-wise operations, like modular addition or

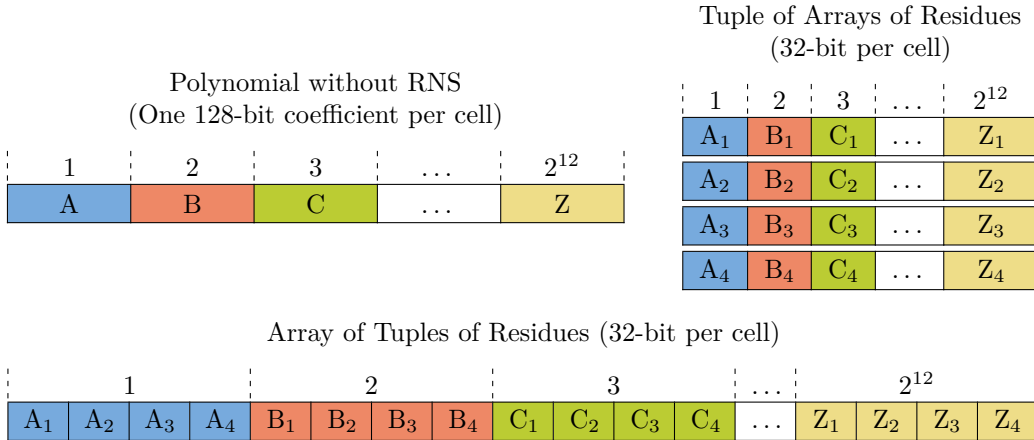


Figure 5: Illustration of different memory layouts for ciphertext polynomials. Shown here for $n = 4096$ and 109-bit coefficients (using 128-bit or 4×32 -bit data types). Residues with the same subscript share the same modulus and are thus assigned to the same DPU (see Subsection 3.3). DRAMatic uses the tuple of arrays of residues layout (top right).

multiplication, as these operations are easily parallelizable and require little synchronization between threads. For more complex operations, like NTT and iNTT, we use coarse-grained multi-threading instead, which avoids synchronization overhead. This can limit performance when operating on only a few sub-polynomials. However, in a typical HE workload, all incoming data and all results are transformed in bulk via NTT and iNTT respectively, which means that NTT operations with few sub-polynomials should be rare.

For the CPU-DPU interface, we use a single MRAM symbol. The memory at this symbol begins with a header, followed by the *main data* — an array of DPU words that spans the rest of the DPU’s MRAM. The header contains information about the rest of the data, like the polynomial length, the modulus, and the number of commands. It also contains some pre-computed data, like the modular inverse of the polynomial length, which is needed to scale down the results of an iNTT. Lastly, the header contains offsets into the *main data*, which define where different data sections start, like the twiddle factors, the commands, or the sub-polynomials to operate on. See Figure 6 for a visualization. This design is very flexible because it allows the host to dynamically define the positions and sizes of the various data sections. It also allows the host to update multiple of these sections in a single data transfer.

Because of the interface design, DRAMatic has low memory overhead on DPUs, only about the size of two sub-polynomials. It consists mainly of the twiddle factors and (to a lesser degree) the interface header. DRAMatic can fill the rest of each DPU’s 60 MB memory³ with sub-polynomials. For a polynomial length of 4096, this means that DRAMatic can store about 3750 sub-polynomials per DPU, which corresponds to 1875 ciphertexts. For a length of 8192, these numbers are halved, *i.e.*, only 1875 sub-polynomials (937 ciphertexts), etc.

4 Evaluation

We first evaluate DRAMatic’s performance compared to previous work, which also implements NTT operations on UPMEM PIM [MHY⁺24], which we will refer to as *MHY⁺*.

³DPU have 64 MB of MRAM, but the UPMEM runtime requires some memory for itself, as well as for logging functions like `printf`. We reserve 4 MB for this use (about 6%).

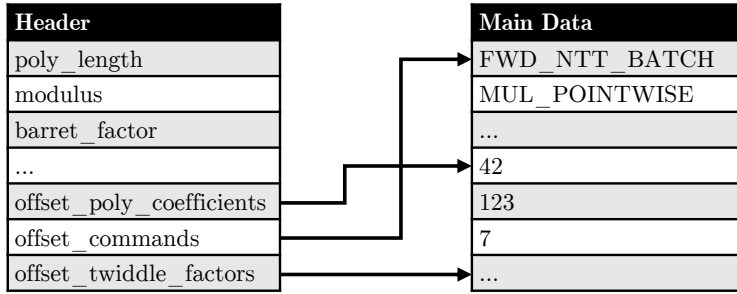


Figure 6: Visualization of the CPU-DPU interface memory layout. The main data immediately follows the header and spans the rest of the DPU’s MRAM.

Both implementations run on our PIM test machine, which is equipped with two Intel® Xeon® Silver 4216 CPUs, 256 GB of standard DDR4 memory, and 4 UPMEM PIM DIMMs with a total capacity of 32 GB, 8 DPU ranks, and 512 DPUs (509 usable). In addition to measuring execution time, we also measure the power consumption of the machine using a GUDE Expert Power Control 8221 metered Power Distribution Unit (PDU). This PDU measures the power consumption “at the wall”, *i.e.*, full system power, including power conversion losses. A significant difference between MHY⁺ and DRAMatic, is that MHY⁺ offloads individual NTT stages onto DPUs, which has large copying and synchronization overhead, while DRAMatic instead offloads the whole NTT operation at once. DRAMatic also utilizes the techniques described above, like RNS, custom multiplications and careful MRAM buffering, to improve performance. We test both implementations with 128 DPUs and a polynomial length of 2048, with a corresponding coefficient size of 54-bit⁴. We do not test longer polynomials, because MHY⁺ only supports NTT on coefficients up to 64-bit, which also limits the operations that can be homomorphically evaluated (see Subsection 6.1). DRAMatic does not have this limitation, but we use the same parameters here for comparability.

Figure 7 (left) shows the NTT performance of DRAMatic and MHY⁺ for different numbers of ciphertexts. When transforming just a single ciphertext, the two implementations are similar in pure computation time; MHY⁺ takes 40 ms, while DRAMatic takes 42 ms. However, DRAMatic’s transfer and retrieval overhead is 36 times lower at 0.5 ms compared to MHY⁺’s 18 ms. If we include this transfer and retrieval overhead, then DRAMatic is 1.4 times faster than MHY⁺, even for a single ciphertext. The reason for this difference is that DRAMatic offloads the whole NTT operation at once, while MHY⁺ instead offloads individual NTT stages.

A bigger difference arises when transforming multiple ciphertexts at once. MHY⁺ uses all available DPUs even for a single ciphertext and its computation time thus rises linearly with the number of ciphertexts to be transformed. DRAMatic instead performs the whole operation on individual DPUs and can thus assign the additional ciphertexts to new DPUs that were previously unutilized. As such, the computation time for DRAMatic stays low as the number of ciphertexts increases, until the 128 DPUs are fully utilized. As a result, DRAMatic gains more of an advantage when more ciphertexts can be processed in parallel. With four ciphertexts, DRAMatic is already 3.8 times faster in pure computation time. And for 64 ciphertexts, DRAMatic is 60.6 times faster than MHY⁺. This scaling levels out at 512 ciphertexts when all 128 DPUs are fully utilized, as shown in Figure 7 (right). For 512 ciphertexts and above, DRAMatic is about 334 times faster in pure computation time. The transfer and retrieve times also scale better for DRAMatic and are about 630 times

⁴This combination achieves 128-bit security according to the Homomorphic Encryption Standard [ACC⁺18]

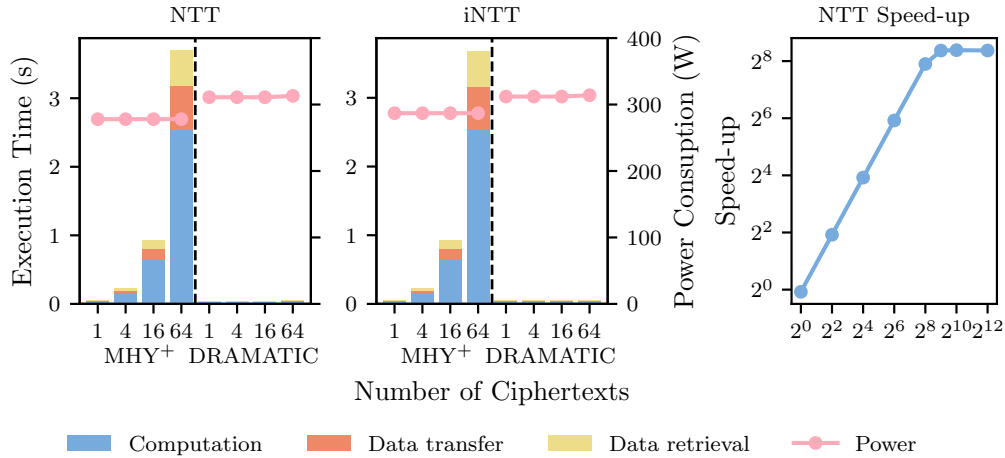


Figure 7: NTT and iNTT performance of DRAMatic compared to previous work [MHY⁺24]. Shown for different numbers of ciphertexts. The log-log plot (right) shows how the speed-up of DRAMatic increases until 2^9 ciphertexts.

faster than MHY⁺ for large numbers of ciphertexts. In relative terms, compared to the pure computation time, MHY⁺ has transfer and retrieve overheads of about 25% and 20% respectively, while DRAMatic reduces these overheads to only 7% and 16% respectively. If we include these transfer and retrieval overheads, then DRAMatic is about 380 times faster than MHY⁺ for 512 ciphertexts and above.

We can see that the power consumption of MHY⁺ stays at a constant 278 watts during these tests, which is expected, since MHY⁺ runs at fixed parallelism and only the amount of work (number of ciphertexts) is changed. DRAMatic instead slightly increases its power consumption from 311 watts up to 323 watts as the number of ciphertexts (and thus DPU utilization) increases. Interestingly, the power consumption is always slightly higher for DRAMatic than for MHY⁺, even though DRAMatic scales its DPU usage while MHY⁺ always uses all DPUs. One reason for this could be that MHY⁺'s synchronization overhead causes more idle time for DPUs or other system components, which lowers their power consumption. Nevertheless, even though DRAMatic has slightly higher power consumption, it is still more energy efficient than MHY⁺, because its execution time is significantly shorter. For 512 ciphertexts and above, DRAMatic uses about 284 times less energy than MHY⁺ for pure computation and about 330 times less energy when including data transfer and retrieval.

DRAMatic also scales better with available parallelism than MHY⁺. When using 256 DPUs instead of 128, the pure computation time for NTT with 4096 ciphertexts drops by 50% for DRAMatic. If we account for the transfer and retrieval overhead, the total time still drops by 46%. In contrast, MHY⁺ cannot effectively use the additional DPUs and even becomes 8% slower due to additional transfer and retrieval overhead. DRAMatic's performance roughly doubles again if we use all 509 DPUs available on our PIM test machine, while MHY⁺ is limited to 256 DPUs, because it requires the number of DPUs to be a power of two.

4.1 Comparing with Microsoft SEAL

We now evaluate the performance of DRAMatic compared to Microsoft SEAL [SEA23], an optimized HE implementation for CPUs, regarding both runtime and energy efficiency. Our PIM test machine, which runs DRAMatic, is the same as above. Our SEAL test

machine is equipped with an Intel® Xeon® Gold 5415+ CPU and 128 GB of DDR5 memory. On this machine, we run SEAL version 4.1.2 compiled with clang-12 using the project’s default CMake Release target. We also measure the power consumption of the SEAL machine using a GUDE Expert Power Control 8035 metered PDU, which again measures full system power.

4.2 Scaling with Polynomial Length

First, we compare the performance and scaling of DRAMatic and SEAL for different polynomial lengths from 1024 up to 8192, with the number of ciphertexts fixed to 32768. We use SEAL’s default coefficient sizes, which aim to achieve 128-bit security for the given polynomial length according to the Homomorphic Encryption Standard [ACC⁺18]. Concretely, we use 27-bit coefficients for polynomials of length 1024, 54-bit coefficients for length 2048, 109-bit coefficients for length 4096, and 218-bit coefficients for length 8192. Note that due to BGV’s modulus switching, these coefficients can also be smaller for some operations. The SEAL machine runs at its maximum parallelism for these tests (16 threads) and the PIM machine utilizes 6 DPU ranks (383 DPUs). The results for NTT, iNTT and BGV multiplication are shown in Figure 8.

On the left of Figure 8, we can see that for both implementations, the NTT execution time increases quadratically with longer polynomial lengths and the correspondingly larger coefficients. However, SEAL performs better in general and is about 7 times faster than DRAMatic in pure computation time. Compared to MHY⁺, this is a significant improvement. MHY⁺ is about 8600 times slower than SEAL in supported configurations (polynomial length of 2048), while DRAMatic closes the gap and is only about 7 times slower than SEAL in this test (using 383 DPUs). We also measure the time required to transfer and retrieve the test data and results from the DPUs. In this test, the transfer and retrieval overhead of DRAMatic is about 7% and 16% respectively. Note however that in a real use-case, the data retrieval step is not necessary directly after an NTT, as the result would typically be the basis for further computations, and only the final results would be retrieved. If the host actually requires the result of an NTT, it should compute the NTT itself, because, as we have seen, SEAL is still faster here. A more realistic scenario with combined NTT, BGV multiplication, and iNTT is shown below. We can also see that the power consumption of both systems stays almost constant during these tests, which is expected, since they both run at fixed parallelism and only the amount of work (length of polynomials and coefficients) is changed. However, the PIM system uses about 62% more power than the SEAL system in these tests. If we account for the computation time, this shows that DRAMatic consumes about 10 times more energy than SEAL for the tested NTT operations, a significant decrease from MHY⁺, which required about 10700 times more energy than SEAL in supported configurations.

The iNTT results (in the middle of Figure 8) are very similar to the NTT results. However, the BGV multiplication tests (on the right of Figure 8) show some differences. Notice that the data transfer and retrieval steps now take up a much larger share of the total execution time on DPUs. Their overhead compared to the pure computation is about 42% and 73% respectively. This indicates that BGV multiplication has lower arithmetic intensity than NTT/iNTT. DRAMatic also performs better in this test and is only about 3 times slower than SEAL in pure computation time. As the power consumption is similar to before, DRAMatic’s energy consumption in this test is thus also only 4.8 times higher than SEAL’s. Execution time still scales quadratically with polynomial length and the corresponding coefficient sizes.

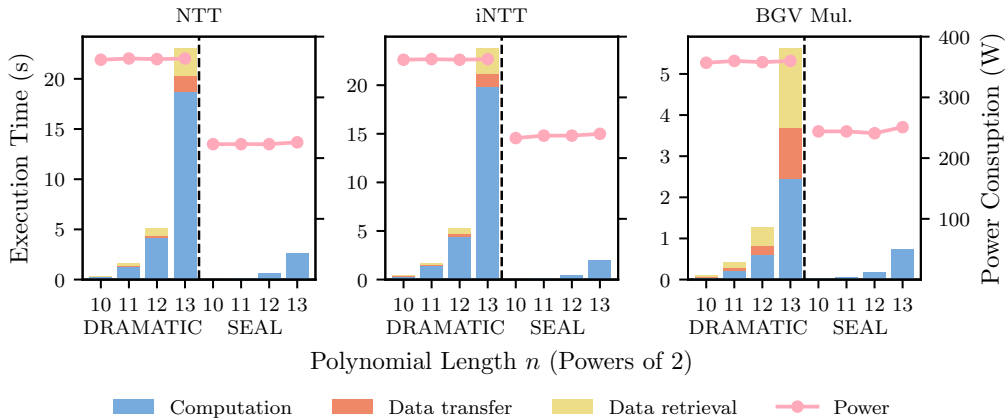


Figure 8: Performance of DRAMatic (DPU) compared to SEAL (CPU).

4.3 Scaling with the Number of Ciphertexts

We now fix the polynomial length to 4096 and test combined NTT, BGV multiplication, and iNTT operations for different numbers of ciphertexts and different levels of parallelism. Figure 9 (left) shows predictable, linear scaling for both implementations as the number of ciphertexts increases. In this combined NTT, BGV multiplication, and iNTT test, we can now take a closer look at DRAMatic’s data transfer and retrieval overhead. They are reduced to about 3% and 6% respectively. In pure computation time, DRAMatic is about 6 times slower than SEAL in these tests. Accounting for the data transfer and retrieval overhead, it is about 7 times slower. Additionally, the SEAL system still uses about 38% less power than the PIM system in these tests.

4.4 Scaling with Available Parallelism

Figure 9 (right) shows how DRAMatic scales with available parallelism compared to SEAL. This is achieved by limiting the number of threads on the SEAL system and the number of DPUs on the PIM system in proportional steps. Note that on the PIM system this is done by limiting the number of ranks used, which is why the number of DPUs must be a multiple of 64 (or close to it, since some ranks contain a few defective DPUs). Because DRAMatic splits moduli over whole DPU ranks, it can only fully utilize the available ranks if they are a multiple of the number of moduli. For the fixed polynomial length of 4096 in these tests, this requires multiples of 3, *i.e.*, 3 or 6 ranks. To provide additional data points at 2, 4 and 8 ranks, we also employ an alternative implementation, in which moduli are processed sequentially using all DPUs. This sequential implementation is marked as bold in the results. Note that the sequential implementation is slightly less efficient than our parallel DRAMatic implementation for numbers of DPUs which both can utilize (192 and 383), as can be seen in Figure 9 (right). However this difference is quite small and the sequential implementation provides good approximations for the available performance with 128, 256, and 509 DPUs.

We can see that the execution times of both systems scale effectively with an increasing number of cores, while the power consumption moderately increases. This is a significant advantage compared to MHY⁺, which cannot effectively use more than 128 DPUs for NTT, and also compared to concurrent work [BMP⁺26], which is limited to 256 DPUs. Note that for the SEAL system, the scaling effectivity becomes weaker once the number of threads exceeds the number of physical cores (8) and they start relying on simultaneous

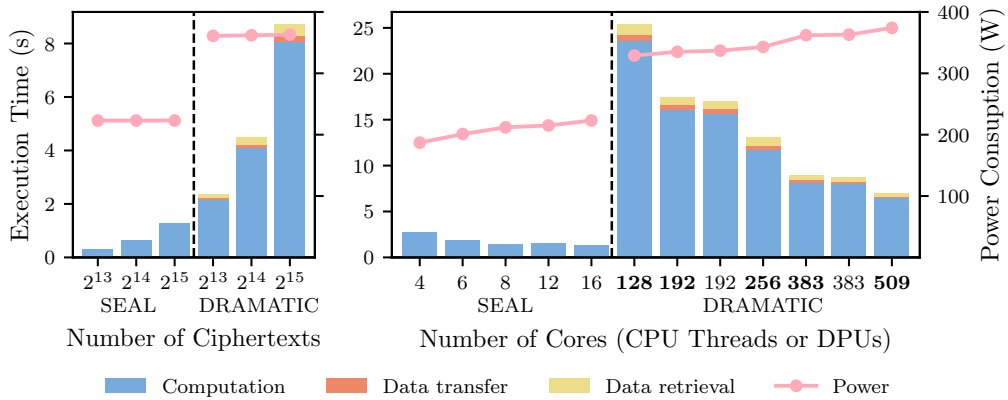


Figure 9: Combined NTT, BGV multiplication, and iNTT performance of DRAMatic (DPU) compared to SEAL (CPU). Shown for different numbers of ciphertexts (left) and different levels of parallelism (right). Bold datapoints use DRAMatic’s sequential implementation (see Subsection 4.4).

multi-threading (SMT). Interestingly, the relative increase in power consumption is lower for the PIM system than for the SEAL system. When going from 2 DPU ranks at 329 watts to 8 DPU ranks at 374 watts, the PIM system becomes 3.7 times faster (in computation time), while only consuming 14% more power. The SEAL system, when going from 4 threads to 16 threads, becomes only about 2.1 times faster, but increases its power consumption by 19% from 187 watts to 223 watts. This difference highlights the high baseline power consumption of the PIM system, which uses about 310 watts even when idle. One reason for this could be the limiting of C-states, which is a step that the UPMEM documentation lists as part of the server installation [UPM25]. We suspect that this step might be required for stability reasons and that the energy efficiency could potentially be improved in future UPMEM products. The limiting of C-states also suggests that UPMEM PIM could be more energy efficient for larger systems with more DPU ranks per CPU or if the CPU is simultaneously used for other tasks.

5 Boosting Performance with Hardware Extensions

We now discuss what hardware limitations are constraining DRAMatic’s performance and what hardware extensions could enable it to further catch up with optimized CPU implementations like SEAL.

5.1 The Multiplication Bottleneck

A major bottleneck for DRAMatic is the weak multiplication performance of DPUs. The DPU hardware only supports 8x8-bit multiplications and bigger multiplications need to be realized in software. Although we leverage RNS representations to minimize the size of datatypes and implement optimized multiplication routines, the coefficient multiplications remain expensive on DPUs. Even our most optimized 32-bit multiplication (with a 32-bit result) takes 21 cycles on a DPU. For comparison, modern CPUs can perform these multiplications in a single cycle, or even perform multiple such operations at the same time using instruction-level parallelism or SIMD instructions.

To gauge the potential performance improvement that would result from faster multiplications on DPUs, we run additional tests in which we replace the multiplication routines

with fast dummy routines, which are about 9- to 10 times faster. Our dummy 32-bit to 32-bit multiplication computes $(a + b) \oplus 12345678_{16}$ in 2 cycles, instead of the 21 cycles needed for proper multiplication. And our dummy 32-bit to 64-bit multiplication computes $a \cdot 2^{20} + b$ in 4 cycles, instead of the normal 35 cycles.

For NTT, the dummy multiplication brings a 2.7 times speed-up. With this fast dummy multiplication, DRAMatic would thus only be around 2.2 times slower than SEAL in pure computation, as shown in Figure 10 (left). The iNTT tests behave similarly, achieving a 2.8 times speed-up. Of the tested operations, BGV multiplication benefits the most from these faster dummy multiplications. It achieves a 3.3 times speed-up and is thus even 1.3 times faster than SEAL in pure computation, as shown in Figure 10 (middle). Note that the data transfer and retrieval overheads stay the same as in earlier tests and thus become more significant as the pure computation time decreases. In the BGV multiplication test, the transfer and retrieval overheads dominate the total runtime at 150% and 270% respectively. In the combined NTT, BGV multiplication, and iNTT tests, which depict these overheads in a more realistic scenario, the transfer and retrieval overhead are reduced to 10% and 18% respectively, as shown in Figure 10 (right). The total speed-up due to the dummy multiplications is about 2.8 times in the combined test, as the NTT and iNTT steps outweigh the BGV multiplication step. DRAMatic would thus only be about 1.9 times slower than SEAL in the combined test.

We also test more optimistic dummy routines that simulate multiplications (both 32-bit to 32-bit and 32-bit to 64-bit) in only one clock cycle, which approaches the speed of modern CPUs⁵. In reality, these dummy routines compute $a + b$ and $(a + b) \cdot 2^{32} + a$ respectively and are inlined at call sites to prevent function call overhead. When testing with these more optimistic dummy routines, the gap between DRAMatic and SEAL almost completely closes. For NTT, the more optimistic dummy routines bring another 1.8 times speed-up, making DRAMatic only 1.2 times slower than SEAL in pure computation. Similarly for iNTT, we would achieve an additional 1.7 times speed-up. For BGV multiplication, the speed-up is 1.8 times, which would make DRAMatic 2.8 times faster than SEAL in pure computation. In the combined NTT, BGV multiplication, and iNTT tests, the gap in computation time is almost closed, as DRAMatic remains only 7% slower than SEAL. However, as the data transfer and retrieval overheads stay the same, they become even more significant compared to these lower computation times. For NTT, these overheads are 32% and 65% respectively. For iNTT, they are 30% and 62%. For BGV multiplication, they are 285% and 436%. And for combined NTT, BGV multiplication, and iNTT, the overheads are 17% and 30%.

Note that these tests are only meant to demonstrate potential speed-ups due to faster multiplications on DPUs. They are based on dummy multiplication routines and cannot be used in a real scenario. However, these tests show that the weak multiplication performance of DPUs remains a major bottleneck for DRAMatic and that faster multiplication hardware on DPUs could bring great performance improvements and close the remaining gap between DRAMatic and SEAL.

5.2 Reducing Data Transfer Overhead

Even though DRAMatic reduces the data transfer overhead about 630 times compared to previous work [MHY⁺24], it is still a significant cost, especially if the DPUs' multiplication performance were to improve as simulated above. While DRAMatic's normal transfer and retrieval overhead is about 9% total in a combined NTT, BGV multiplication, and iNTT test (Figure 9), it rises to 28% if we simulate improved DPU multiplication performance (right of Figure 10), or even 47% with the more optimistic dummy routines. With the

⁵Even if DPUs could multiply in one cycle, their clock frequency (400 MHz) is still lower than that of modern CPUs (multiple GHz).

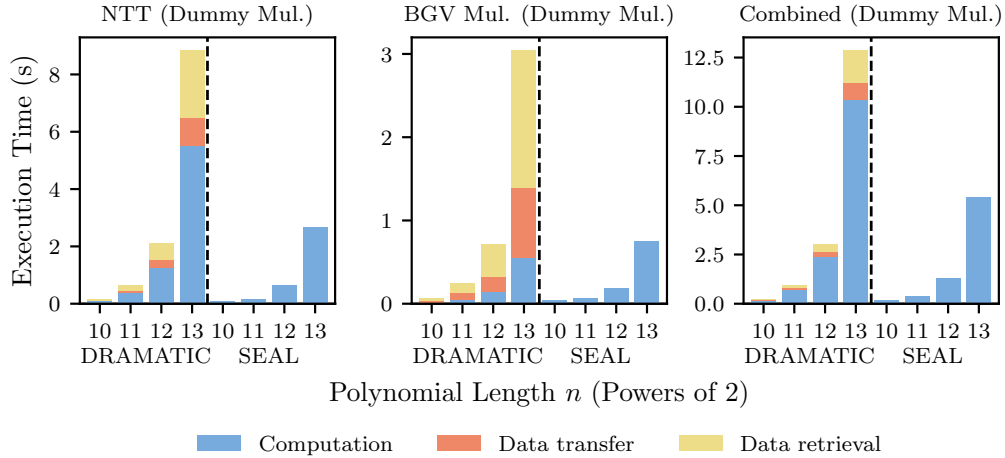


Figure 10: Simulated performance of DRAMatic using dummy multiplications (DPU) compared to SEAL (CPU).

simulated DPU multiplication performance, DRAMatic could be 1.3 times faster than SEAL for pure BGV multiplication, were it not for the significant transfer and retrieval overhead of about 420% total, as shown in Figure 10 (middle). This is especially relevant in this scenario, since we have some operations (NTT/iNTT) which are faster for SEAL, and some operations (BGV multiplication) which are faster for DRAMatic (excluding transfer overhead). If we could overcome the transfer overhead in this scenario, it would enable a form of *hybrid computing* in which the CPU and DPUs work together and each perform the sub-tasks for which they are most suitable, improving overall performance.

However, this is currently not possible with UPMEM PIM, as the CPU cannot operate normally on the memory of the PIM DIMMs. Instead, the CPU must use normal DRAM for its computations and then copy the data to the PIM DIMMs, when work should be offloaded to DPUs. This is required, in part, because the memory chips on DIMMs are interleaved, *i.e.*, logically consecutive bytes are stored in separate DRAM-chips. The data must thus be transposed when making it available to DPUs, as they can only access one DRAM-chip each. This transposition is done automatically by the UPMEM runtime, but it requires copying the data.

UPMEM PIM is most suited for operations with large amounts of data and low arithmetic-intensity, as it removes the bottleneck of getting the data from memory to the processing units. However, if the data is dynamic, then these operations also have the most substantial copying overhead, as the data must be copied to the DPUs every time. In this case, it is faster to perform the computations directly on the CPU, since the data must be read anyway to copy it. To improve the performance of UPMEM PIM in these use-cases with frequently changing data, like HE, we propose a hybrid computing system, which allows the CPU to use the DPUs memory directly when the DPUs are not currently active. This hybrid system would allow DPUs to immediately continue a computation whose previous steps were performed by the CPU, as long as the CPU finishes its computation with the proper memory transposition. In many cases, this transposition could also be combined with the main computation, without requiring an additional pass over the data, or copying it. This proposed change could greatly reduce the data transfer overhead and would make UPMEM PIM behave more like memory that can also compute, instead of a discrete accelerator that data must be transferred to.

6 Related Work

We classify the related work into categories: Works that use UPMEM PIM for accelerating HE or NTT, works that use UPMEM PIM in other cryptographic contexts, works that accelerate HE using other PIM systems, and works that accelerate HE without using PIM.

6.1 Using UPMEM PIM for Accelerating HE

Previous work [MHY⁺24], which we compared against in Section 4, has also explored using UPMEM PIM for accelerating HE. They implement polynomial addition and multiplication on UPMEM PIM and integrate their implementation with the OpenFHE library [BAB²²] using its hardware abstraction layer (HAL). However, this HAL-based integration offloads many small (sub)-operations to DPUs, instead of the larger overarching operation as a whole. Especially for NTT, this requires many copy operations between the DPUs and the host, as well as complex synchronization, as NTT stages are offloaded individually. In this work, we instead implement NTT on the DPUs directly and offload the whole operation at once. This saves the expensive copying and synchronization operations and enables better parallelism and further DPU-centric optimizations.

Additionally, for some operations, MHY⁺ only measure their performance on 16-bit coefficients, which are too small for practical HE use. In this work, we instead test with larger, more realistic coefficients sizes and also implement custom multiplication routines to speed-up operations on these larger coefficients. The maximum coefficient size of MHY⁺ is also limited to 64-bit, which greatly constrains the operations that can be homomorphically evaluated, as coefficient size is tied to the noise-budget and thus the maximum multiplicative depth of HE operations (or bootstrapping frequency for FHE). According to the Homomorphic Encryption Standard [ACC¹⁸], this maximum coefficient size corresponds to a polynomial length of 2048 for 128-bit security. However, most non-trivial homomorphic evaluations require larger parameters. For example, in homomorphic matrix multiplications [JKLS18, RT22] the matrix sizes are limited by the number of *slots* which is proportional to the polynomial length. With $n=2048$, previous work [MHY⁺24] is thus limited to square matrix dimensions of 32, while DRAMatic can support larger matrices. As another example, Homomorphic Evaluation of the AES Circuit [GHS12] requires modulus sizes of 493 bits with bootstrapping or 886 bits for all ten rounds without bootstrapping. Such a computation thus cannot be performed with MHY⁺, as it is limited to 64-bit coefficients. In contrast, DRAMatic does support these parameters and can be used to securely perform these non-trivial homomorphic evaluations.

6.2 Using UPMEM PIM for HE-suitable NTT

Concurrent work [BMP⁺26], which we will refer to as *BMP⁺*, has also investigated optimized NTT implementations on UPMEM PIM, specifically for large parameters as required by some FHE use-cases. They compare different modular reductions (Barret and Montgomery), radices, and NTT algorithms, which they call 1D NTT, 2D NTT, and 4D NTT. But unlike DRAMatic, they do not implement other polynomial operations or HE multiplication (*e.g.*, BGV). DRAMatic’s NTT implementation is similar to their 1D NTT approach (using Barret reduction).

Unfortunately, the implementation of *BMP⁺* is currently not publicly available. However, we attempt to recreate the test conditions from their work (2^{16} polynomial length, 1241-bit coefficients, and 256 DPUs). With DRAMatic’s NTT implementation, this takes about 32.6 ms per polynomial (averaged over 4096 polynomials that are transformed in parallel, including data transfer and retrieval overhead). For comparison, the 1D NTT_v2 Barret variant of *BMP⁺* takes 43.2 ms per polynomial, so DRAMatic’s 1D NTT implementation is about 33% faster. However, their alternative 2D NTT Barret variant only

takes 25.3 ms per polynomial, which would be 29% faster than DRAMatic, as DRAMatic does not currently support 2D NTT. Their 4D NTT takes between 28.1 ms and 20.5 ms per polynomial based on the radix used, so it could be up to 59% faster than DRAMatic’s 1D NTT in this use case. They also present NTT variants that use Montgomery reduction and achieve further improvements, but these are not directly comparable with DRAMatic, as they require pre-transforming the values into Montgomery space.

In addition to these differences, BMP^+ also requires specific DPU counts⁶, while DRAMatic is more flexible and can utilize both larger and smaller DPU installations. For example, using all 509 DPUs of our PIM test machine, DRAMatic’s NTT time drops to 23 ms per polynomial, comparable to BMP^+ ’s 4D NTT that is limited to 256 DPUs. Lastly, due to DRAMatic’s coarse-grained multi-threading for NTT, it requires larger workloads (multiple ciphertexts) to reach its full performance (see for example Figure 7), while BMP^+ can also efficiently operate on single ciphertexts/polynomials. In the future, it could be interesting to investigate whether DRAMatic’s optimizations can be combined with the 2D or 4D NTT approach of BMP^+ .

6.3 Using UPMEM PIM for other Cryptography

A different approach to secure computing on UPMEM PIM was investigated by [GZS25]. Instead of using HE like in this work, they leverage multi-party computation (MPC) techniques to integrate PIM modules within a secure computing system by protecting the data as it moves off-chip to the PIM modules.

6.4 Accelerating HE using other PIM Systems

In [GR21], the authors design custom PIM hardware for accelerating HE, and evaluate its performance using a simulator, which shows a large theoretical speed-up compared to CPU implementations. This is fundamentally different from our work, since they evaluate custom hardware designs and simulate them, while we instead implement and evaluate HE operations on real general-purpose PIM hardware.

6.5 Accelerating HE without PIM

Lastly, there has also been extensive research into accelerating HE on other computing architectures, separate from PIM. There are popular CPU implementations like OpenFHE [BAB⁺22] and Microsoft SEAL [SEA23], which we also compared against, as well as optimized implementations for GPUs [JKA⁺21] and FPGAs [PNPM15].

7 Conclusion

We presented DRAMatic, which implements efficient polynomial operations and NTT directly on UPMEM PIM DPUs, as the basis for HE operations. DRAMatic supports large parameter sizes, as required for practical, secure homomorphic evaluations. We addressed the unique challenges of the UPMEM PIM platform by implementing DPU-centric optimizations, like custom multiplication routines, and by considering efficient data layouts. Our results show promising scaling with increasing parallelism and a 334 times speed-up compared to previous work on accelerating HE with UPMEM PIM [MHY⁺24], significantly closing the gap to optimized CPU implementations. Our experiments indicated that the weak multiplication performance of DPUs remains a bottleneck and that DRAMatic has not fully caught up with libraries like Microsoft SEAL. We thus proposed hardware

⁶In their journal pre-proof, they state that they selected 256 DPUs, as otherwise not all of their kernels can be implemented.

extensions to UPMEM PIM, which could eliminate these bottlenecks and further improve DRAMatic’s performance. Compared to concurrent work on accelerating NTT execution on UPMEM PIM [BMP⁺26], we showed that our NTT implementation scales better with more DPUs and is 33% faster than the directly comparable 1D NTT. However, DRAMatic does not currently support 2D NTT or 4D NTT, which show even better performance. Lastly, we measured and evaluated the power consumption of our test systems and showed that the UPMEM PIM system is less energy efficient than the CPU system. However, the scaling of power consumption with increasing parallelism looks promising for UPMEM PIM and could benefit larger PIM installations.

8 Future Work

Future research could focus on integrating our proposed hardware extensions and hybrid computing architecture into UPMEM PIM or similar processing-in-memory platforms. A key area of interest is the potential synergy between DRAMatic’s optimizations and recent 2D/4D NTT approaches [BMP⁺26] to further enhance throughput. Achieving efficient bootstrapping remains a critical milestone to enable full FHE support on UPMEM PIM. Finally, investigating the portability of these optimizations to other programmable PIM architectures, such as AxDIMM [KZS⁺22], will provide insights into the broader applicability of our acceleration techniques.

Acknowledgments

Generative AI was utilized to generate plots, for editing, and for grammar enhancement of this work. This work has been supported by the BMFTR through the project AnoMed.

References

- [ACC⁺18] Martin Albrecht, Melissa Chase, Hao Chen, Jintai Ding, Shafi Goldwasser, Sergey Gorbunov, Shai Halevi, Jeffrey Hoffstein, Kim Laine, Kristin Lauter, Satya Lokam, Daniele Micciancio, Dustin Moody, Travis Morrison, Amit Sahai, and Vinod Vaikuntanathan. Homomorphic encryption security standard. Technical report, HomomorphicEncryption.org, Toronto, Canada, November 2018.
- [BAB⁺22] Ahmad Al Badawi, Andreea Alexandru, Jack Bates, Flavio Bergamaschi, David Bruce Cousins, Saroja Erabelli, Nicholas Genise, Shai Halevi, Hamish Hunt, Andrey Kim, Yongwoo Lee, Zeyu Liu, Daniele Micciancio, Carlo Pascoe, Yuriy Polyakov, Ian Quah, Saraswathy R. V., Kurt Rohloff, Jonathan Saylor, Dmitriy Suponitsky, Matthew Triplett, Vinod Vaikuntanathan, and Vincent Zucca. OpenFHE: Open-source fully homomorphic encryption library. Cryptology ePrint Archive, Report 2022/915, 2022. URL: <https://eprint.iacr.org/2022/915>.
- [Bar87] Paul Barrett. Implementing the Rivest Shamir and Adleman public key encryption algorithm on a standard digital signal processor. In Andrew M. Odlyzko, editor, *CRYPTO’86*, volume 263 of *LNCS*, pages 311–323. Springer, Berlin, Heidelberg, August 1987. doi:[10.1007/3-540-47721-7_24](https://doi.org/10.1007/3-540-47721-7_24).
- [BGV12] Zvika Brakerski, Craig Gentry, and Vinod Vaikuntanathan. (Leveled) fully homomorphic encryption without bootstrapping. In Shafi Goldwasser, editor,

ITCS 2012, pages 309–325. ACM, January 2012. [doi:10.1145/2090236.2090262](https://doi.org/10.1145/2090236.2090262).

[BMP⁺26] Tathagata Barik, Priyam Mehta, Zaira Pindado, Harshita Gupta, Mayank Kabra, Mohammad Sadrosadati, Onur Mutlu, and Antonio J. Peña. Long integer NTT execution on UPMEM-PIM for 128-bit secure fully homomorphic encryption. *Future Generation Computer Systems*, page 108386, 2026. URL: <https://www.sciencedirect.com/science/article/pii/S0167739X2600208>, [doi:10.1016/j.future.2026.108386](https://doi.org/10.1016/j.future.2026.108386).

[Bra12] Zvika Brakerski. Fully homomorphic encryption without modulus switching from classical GapSVP. In Reihaneh Safavi-Naini and Ran Canetti, editors, *CRYPTO 2012*, volume 7417 of *LNCS*, pages 868–886. Springer, Berlin, Heidelberg, August 2012. [doi:10.1007/978-3-642-32009-5_50](https://doi.org/10.1007/978-3-642-32009-5_50).

[CGGI20] Ilaria Chillotti, Nicolas Gama, Mariya Georgieva, and Malika Izabachène. TFHE: Fast fully homomorphic encryption over the torus. *Journal of Cryptology*, 33(1):34–91, January 2020. [doi:10.1007/s00145-019-09319-x](https://doi.org/10.1007/s00145-019-09319-x).

[CKKS17] Jung Hee Cheon, Andrey Kim, Miran Kim, and Yong Soo Song. Homomorphic encryption for arithmetic of approximate numbers. In Tsuyoshi Takagi and Thomas Peyrin, editors, *ASIACRYPT 2017, Part I*, volume 10624 of *LNCS*, pages 409–437. Springer, Cham, December 2017. [doi:10.1007/978-3-319-70694-8_15](https://doi.org/10.1007/978-3-319-70694-8_15).

[CSB⁺26] Jalen Chuang, Alex Seto, Nicolas Berrios, Stephan van Schaik, Christina Garman, and Daniel Genkin. TEE.fail: Breaking trusted execution environments via DDR5 memory bus interposition. In *47th IEEE Symposium on Security and Privacy*. IEEE Computer Society, 2026. URL: <https://tee.fail>.

[CT65] James W. Cooley and John W. Tukey. An algorithm for the machine calculation of complex Fourier series. *Mathematics of computation*, 19(90):297–301, 1965.

[dCAY⁺21] Leo de Castro, Rashmi Agrawal, Rabia Yazicigil, Anantha Chandrakasan, Vinod Vaikuntanathan, Chiraag Juvekar, and Ajay Joshi. Does fully homomorphic encryption need compute acceleration? Cryptology ePrint Archive, Report 2021/1636, 2021. URL: <https://eprint.iacr.org/2021/1636>.

[FV12] Junfeng Fan and Frederik Vercauteren. Somewhat practical fully homomorphic encryption. Cryptology ePrint Archive, Report 2012/144, 2012. URL: <https://eprint.iacr.org/2012/144>.

[GBK⁺19] Saugata Ghose, Amirali Boroumand, Jeremie S Kim, Juan Gómez-Luna, and Onur Mutlu. Processing-in-memory: A workload-driven perspective. *IBM Journal of Research and Development*, 63(6):3–1, 2019.

[GHF⁺21] Juan Gómez-Luna, Izzat El Hajj, Ivan Fernandez, Christina Giannoula, Geraldo F. Oliveira, and Onur Mutlu. Benchmarking a new paradigm: An experimental analysis of a real processing-in-memory architecture. *CoRR*, abs/2105.03814, 2021. URL: <https://arxiv.org/abs/2105.03814>, [arXiv:2105.03814](https://arxiv.org/abs/2105.03814).

[GHS12] Craig Gentry, Shai Halevi, and Nigel P. Smart. Homomorphic evaluation of the AES circuit. In Reihaneh Safavi-Naini and Ran Canetti, editors, *CRYPTO 2012*, volume 7417 of *LNCS*, pages 850–867. Springer, Berlin, Heidelberg, August 2012. [doi:10.1007/978-3-642-32009-5_49](https://doi.org/10.1007/978-3-642-32009-5_49).

[GR21] Saransh Gupta and Tajana Simunic Rosing. Invited: Accelerating fully homomorphic encryption with processing in memory. In *58th ACM/IEEE Design Automation Conference, DAC 2021, San Francisco, CA, USA, December 5-9, 2021*, pages 1335–1338. IEEE, 2021. [doi:10.1109/DAC18074.2021.9586285](https://doi.org/10.1109/DAC18074.2021.9586285).

[GS66] W. Morven Gentleman and Gordon Sande. Fast Fourier transforms: for fun and profit. In *Proceedings of the November 7-10, 1966, fall joint computer conference*, pages 563–578, 1966.

[GZS25] Sahar Ghoflsaz Ghinani, Jingyao Zhang, and Elaheh Sadredini. Enabling low-cost secure computing on untrusted in-memory architectures. In *Proceedings of the 34th USENIX Conference on Security Symposium, SEC '25, USA, 2025*. USENIX Association.

[HPS19] Shai Halevi, Yuriy Polyakov, and Victor Shoup. An improved RNS variant of the BFV homomorphic encryption scheme. In Mitsuru Matsui, editor, *CT-RSA 2019*, volume 11405 of *LNCS*, pages 83–105. Springer, Cham, March 2019. [doi:10.1007/978-3-030-12612-4_5](https://doi.org/10.1007/978-3-030-12612-4_5).

[JKA⁺21] Wonkyung Jung, Sangpyo Kim, Jung Ho Ahn, Jung Hee Cheon, and Younho Lee. Over 100x faster bootstrapping in fully homomorphic encryption through memory-centric optimization with GPUs. *IACR TCHES*, 2021(4):114–148, 2021. URL: <https://tches.iacr.org/index.php/TCHES/article/view/9062>, [doi:10.46586/tches.v2021.i4.114-148](https://doi.org/10.46586/tches.v2021.i4.114-148).

[JKLS18] Xiaoqian Jiang, Miran Kim, Kristin E. Lauter, and Yongsoo Song. Secure outsourced matrix computation and application to neural networks. In David Lie, Mohammad Mannan, Michael Backes, and XiaoFeng Wang, editors, *ACM CCS 2018*, pages 1209–1222. ACM Press, October 2018. [doi:10.1145/3243734.3243837](https://doi.org/10.1145/3243734.3243837).

[KZS⁺22] Liu Ke, Xuan Zhang, Jinin So, Jong-Geon Lee, Shinhaeng Kang, Sukhan Lee, Songyi Han, YeonGon Cho, Jin Hyun Kim, Yongsuk Kwon, KyungSoo Kim, Jin Jung, IlKwon Yun, Sung Joo Park, Hyunsun Park, Joon-Ho Song, Jeonghyeon Cho, Kyomin Sohn, Nam Sung Kim, and Hsien-Hsin S. Lee. Near-memory processing in action: Accelerating personalized recommendation with AxDIMM. *IEEE Micro*, 42(1):116–127, 2022. [doi:10.1109/MM.2021.309770](https://doi.org/10.1109/MM.2021.309770).

[MHY⁺24] Mpoki Mwaisela, Joel Hari, Peterson Yuhala, Jämes Ménétrey, Pascal Felber, and Valerio Schiavoni. Evaluating the potential of in-memory processing to accelerate homomorphic encryption: Practical experience report. In *43rd International Symposium on Reliable Distributed Systems, SRDS 2024, Charlotte, NC, USA, September 30 - Oct. 3, 2024*, pages 92–103. IEEE, 2024. [doi:10.1109/SRDS64841.2024.00019](https://doi.org/10.1109/SRDS64841.2024.00019).

[MIE17] Ahmad Moghimi, Gorka Irazoqui, and Thomas Eisenbarth. CacheZoom: How SGX amplifies the power of cache attacks. In Wieland Fischer and Naofumi Homma, editors, *CHES 2017*, volume 10529 of *LNCS*, pages 69–90. Springer, Cham, September 2017. [doi:10.1007/978-3-319-66787-4_4](https://doi.org/10.1007/978-3-319-66787-4_4).

[PNPM15] Thomas Pöppelmann, Michael Naehrig, Andrew Putnam, and Adrián Macías. Accelerating homomorphic evaluation on reconfigurable hardware. In Tim Güneysu and Helena Handschuh, editors, *CHES 2015*, volume 9293 of *LNCS*, pages 143–163. Springer, Berlin, Heidelberg, September 2015. [doi:10.1007/978-3-662-48324-4_8](https://doi.org/10.1007/978-3-662-48324-4_8).

[RT22] Panagiotis Rizomiliotis and Aikaterini Triakosia. On matrix multiplication with homomorphic encryption. In Francesco Regazzoni and Marten van Dijk, editors, *Proceedings of the 2022 on Cloud Computing Security Workshop, CCSW 2022, Los Angeles, CA, USA, 7 November 2022*, pages 53–61. ACM, 2022. [doi:10.1145/3560810.3564267](https://doi.org/10.1145/3560810.3564267).

[SEA23] Microsoft SEAL (release 4.1). <https://github.com/Microsoft/SEAL>, January 2023. Microsoft Research, Redmond, WA.

[Sho05] Victor Shoup. *A Computational Introduction to Number Theory and Algebra*. Cambridge University Press, 2005.

[SSM⁺23] Ardianto Satriawan, Infall Syafalni, Rella Mareta, Isa Anshori, Wervyan Shalannanda, and Aleams Barra. Conceptual review on number theoretic transform and comprehensive review on its implementations. *IEEE Access*, 11:70288–70316, 2023. [doi:10.1109/ACCESS.2023.3294446](https://doi.org/10.1109/ACCESS.2023.3294446).

[UPM24] UPMEM. Keynote: UPMEM PIM platform for data-intensive applications. Presentation slides, ABUMPIMP 2024 at Euro-Par 2024, 2024.

[UPM25] UPMEM DPU SDK 2025.1.0 documentation — server installation. https://sdk.upmem.com/2025.1.0/280_Server_configuration.html, 2025.

[WSE24] Luca Wilke, Florian Sieck, and Thomas Eisenbarth. TDXdown: Single-stepping and instruction counting attacks against intel TDX. In Bo Luo, Xiaojing Liao, Jun Xu, Engin Kirda, and David Lie, editors, *ACM CCS 2024*, pages 79–93. ACM Press, October 2024. [doi:10.1145/3658644.3690230](https://doi.org/10.1145/3658644.3690230).

[ZNG⁺25] Minxuan Zhou, Yujin Nam, Pranav Gangwar, Weihong Xu, Arpan Dutta, Chris Wilkerson, Rosario Cammarota, Saransh Gupta, and Tajana Rosing. FHEmem: A processing in-memory accelerator for fully homomorphic encryption. *IEEE Transactions on Emerging Topics in Computing*, pages 1–16, 2025. [doi:10.1109/TETC.2025.3528862](https://doi.org/10.1109/TETC.2025.3528862).